Communication

Reversible Formation and Dispersion of Chiral Assemblies Responding to Electron Transfer

Junpei Yuasa, and Shunichi Fukuzumi

J. Am. Chem. Soc., **2007**, 129 (43), 12912-12913• DOI: 10.1021/ja075149q • Publication Date (Web): 06 October 2007

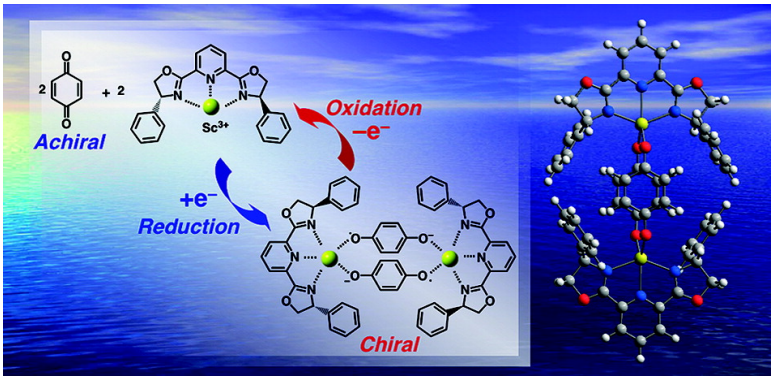

More About This Article

Additional resources and features associated with this article are available within the HTML version:

- Supporting Information
- Access to high resolution figures
- Links to articles and content related to this article
- Copyright permission to reproduce figures and/or text from this article

View the Full Text HTML

J|A|C|S
COMMUNICATIONS

Published on Web 10/06/2007

Reversible Formation and Dispersion of Chiral Assemblies Responding to Electron Transfer

Junpei Yuasa and Shunichi Fukuzumi*

Department of Material and Life Science, Division of Advanced Science and Biotechnology, Graduate School of Engineering, Osaka University, SORST, Japan Science and Technology Agency (JST), Suita, Osaka 565-0871, Japan

Received July 11, 2007; E-mail: fukuzumi@chem.eng.osaka-u.ac.jp

Supramolecular chiral assemblies are widespread and play a crucial role in a variety of biological systems such as the DNA double helix, heme proteins, and the photosynthetic architecture. Those chiral assemblies are achieved by noncovalent interactions between chiral building blocks (e.g., amino acid, nucleic acids, sugars, lipids, etc.), and its chirality is transferred to quaternary structure through noncovalent interactions.[1] The strength of noncovalent interactions in natural systems is often associated with redox reactions, being related to conformational changes of biological macromolecules.[2,3] Effective redox control on building affinity of the chiral supramolecules [e.g., hydrogen bonds[4−7] and metal−ligand interactions][8−11] would ultimately afford reversible formation and dispersion of chiral assemblies in response to a simple external signal such as an electron, giving achiral−chiral switchability.[12]

We report herein reversible formation of a chiral π-dimer complex between *p*-benzosemiquinone radical anions, which are one of the most important biological redox molecules,[13] and a chiral scandium complex of 2,6-bis-(oxazolinyl)pyridine, [Sc-pybox]-$(OTf)_3$ [OTf = OSO_2CF_3][14] in response to a change in the redox state of *p*-benzoquinones.[15,16] Stereochemistry of novel chiral π-dimer complexes assigned by ^{1}H NMR, COSY NMR, and NOE experiments provides valuable insight into how the chirality is transferred from chiral Sc^{3+}-pybox to *p*-benzoquinones with high symmetry through noncovalent interactions.[17]

Upon addition of Sc^{3+}(*R*)-pybox (6.7×10^{-2} M) to a 1:1 mixture of a deaerated acetonitrile (MeCN) solution of *p*-benzoquinone (Q, 3.4×10^{-2} M) and hydroquinone (QH_2, 3.4×10^{-2} M), strong new absorption bands (denoted as $\lambda_H = 376$ and $\lambda_L = 583$ nm) appear as shown in red solid line in Figure 1a.[18,19] When Q and QH_2 are replaced by 1,4-naphthoquinone (NQ) and hydronaphthoquinone (NQH_2), the absorption maxima ($\lambda_H = 376$ and $\lambda_L = 583$ nm) are shifted to $\lambda_H = 422$ and $\lambda_L = 633$ nm, respectively (blue solid line in Figure 1a). Such UV−vis spectral changes are associated with remarkable color changes (shown in photographs in Figure 1b,c).

The circular dichroism (CD) spectra of the quinone−hydroquinone systems were measured in the presence of Sc^{3+}(*R*)-pybox and Sc^{3+}(*S*)-pybox. The results are shown in Figure 1b,c, where the Cotton effects of the CD bands with complete mirror images for their enantiomer pairs are observed. This indicates the chiral organization of the quinone−hydroquinone systems with Sc^{3+}-pybox.

To identify the chiral aggregate, an MeCN solution of NQ (3.0×10^{-4} M) and NQH_2 (3.0×10^{-4} M) in the presence of Sc^{3+}-(*R*)-pybox (6.0×10^{-4}) was examined by positive-ion ESI mass (Figure 1d). The positive-ion ESI mass spectrum shows a signal at *m*/*z* 1591.4, which corresponds to $\{[(NQ^{\bullet-})_2-(Sc^{3+}(R)\text{-pybox})_2(OTf^-)_3]\}^+$. The signal has a characteristic distribution of isotopomers (Figure 1d) that matches well with the calculated isotopic distribution for $\{[(NQ^{\bullet-})_2-(Sc^{3+}(R)\text{-pybox})_2(OTf^-)_3]\}^+$ (Figure 1e). This indicates formation of a 2:2 chiral π-dimer complex of $NQ^{\bullet-}$

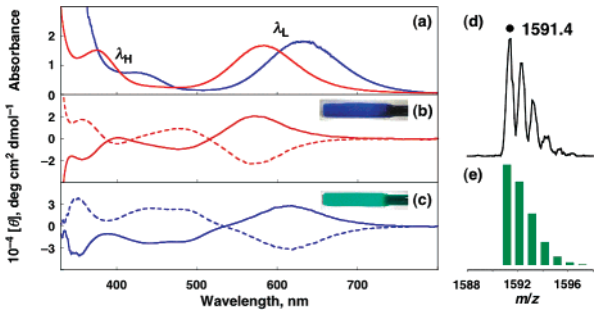

Figure 1. (a) UV−vis spectra of a deaerated MeCN solution of Q (3.4×10^{-2} M) and QH_2 (3.4×10^{-2} M) in the presence of Sc^{3+}(*R*)-pybox (6.7×10^{-2} M) [red solid line], NQ (7.0×10^{-3} M) and NQH_2 (7.0×10^{-3} M) in the presence of Sc^{3+}(*R*)-pybox (1.3×10^{-2} M) [blue solid line] (1 mm path-length). Corresponding CD spectra of (b) Q-QH_2 and (c) NQ-NQH_2 systems in the presence of Sc^{3+}(*R*)-pybox (solid lines) and Sc^{3+}(*S*)-pybox (dashed lines). (d) Positive-ion ESI mass spectrum of an MeCN solution of NQ (3.0×10^{-4} M) and NQH_2 (3.0×10^{-4} M) in the presence of [Sc-(*R*)-pybox](OTf)$_3$ (6.0×10^{-4} M). The signal at *m*/*z* 1591.4 corresponds to $\{[(NQ^{\bullet-})_2-(Sc^{3+}(R)\text{-pybox})_2(OTf^-)_3]\}^+$. (e) Calculated isotopic distributions for $\{[(NQ^{\bullet-})_2-(Sc^{3+}(R)\text{-pybox})_2(OTf^-)_3]\}^+$. The insets show photographs of a deaerated MeCN solution of (b) Q (1.0×10^{-1} M) and QH_2 (1.0×10^{-1} M) in the presence of Sc^{3+}(*R*)-pybox (1.0×10^{-1} M), and (c) NQ (1.0×10^{-1} M) and NQH_2 (1.0×10^{-1} M) in the presence of Sc^{3+}-(*R*)-pybox (1.0×10^{-1} M).

with Sc^{3+}(*R*)-pybox, $[(NQ^{\bullet-})_2-(Sc^{3+}(R)\text{-pybox})_2]$ in the proportionation equilibrium between NQ and NQH_2 in the presence of Sc^{3+}-(*R*)-pybox (eq 1c). The stoichiometry in eq 1c is confirmed by UV−vis and ^{1}H NMR titration (see Supporting Information S2).[19]

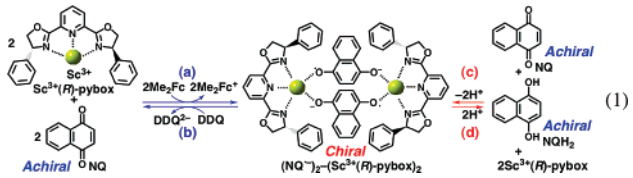

(1)

The chiral π-dimer complexes are also formed by the electron-transfer (ET) reduction of *p*-quinones by electron donors such as 1,1′-dimethylferrocene (Me_2Fc) in the presence of Sc^{3+}(*R*)-pybox (vide infra). The absorption bands due to $(NQ^{\bullet-})_2-(Sc^{3+}(R)\text{-pybox})_2$ are observed upon addition of Me_2Fc (1.7×10^{-3} M) to a deaerated MeCN solution of NQ (6.9×10^{-3} M) in the presence of Sc^{3+}-(*R*)-pybox (1.0×10^{-1} M) [see Supporting Information S3].[20] Those absorption bands completely disappear upon the addition of 2,3-dichloro-5,6-dicyano-*p*-benzoquinone [DDQ (8.5×10^{-4} M)] to the MeCN solution of $(NQ^{\bullet-})_2-(Sc^{3+}(R)\text{-pybox})_2$ (see Supporting Information S3). Since neutral NQ has virtually no interaction with Sc^{3+}(*R*)-pybox,[21] the formation and dispersion of $(NQ^{\bullet-})_2-(Sc^{3+}$-$(R)\text{-pybox})_2$ in response to the ET reduction and oxidation can be expressed by eq 1a and 1b, respectively. The ET reduction of 2 equiv of NQ by 2 equiv of Me_2Fc in the presence of 2 equiv of

10.1021/ja075149q CCC: $37.00

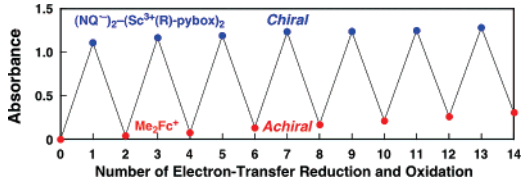

Figure 2. Absorbance at 633 nm for cycles of ET reduction of a deaerated MeCN solution of NQ (6.9×10^{-3} M) and Sc^{3+}(*R*)-pybox (1.0×10^{-1} M) by Me_2Fc (1.7×10^{-3} M) [blue circles] and oxidation by DDQ (8.5×10^{-4} M) [red circles] at 298 K (1 mm path-length).

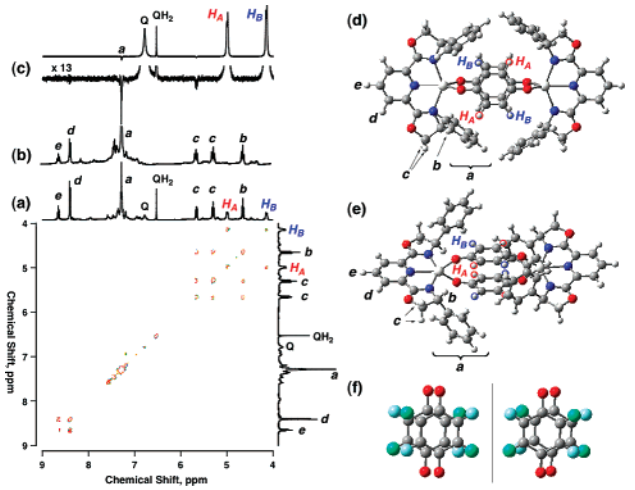

Figure 3. (a) ^{1}H, ^{1}H COSY NMR and (c) NOE NMR spectra of a deaerated CD_3CN solution of Q (5.0×10^{-2} M) and Me_2Fc (5.0×10^{-2} M) in the presence of Sc^{3+}(*R*)-pybox (5.0×10^{-2} M) at 298 K. (b) ^{1}H NMR spectrum of a deaerated CD_3CN solution of Q-d_4 (5.0×10^{-2} M) and Me_2Fc (5.0×10^{-2} M) in the presence of Sc^{3+}(*R*)-pybox (5.0×10^{-2} M) at 298 K. The optimized structure of $(Q^{\bullet-})_2-(Sc^{3+}(R)\text{-pybox})_2$ calculated by using DFT at the B3LYP/6-31G*: top view (d) and front view (e). (f) An enantiomer pair of the $(Q^{\bullet-})_2$ unit in $(Q^{\bullet-})_2-(Sc^{3+}\text{-pybox})_2$.

Sc^{3+}(*R*)-pybox yields 1 equiv of $(NQ^{\bullet-})_2-(Sc^{3+}(R)\text{-pybox})_2$ (eq 1a), while the two-electron oxidation of $(NQ^{\bullet-})_2-(Sc^{3+}(R)\text{-pybox})_2$ by 1 equiv of DDQ results in reproducing NQ and Sc^{3+}(*R*)-pybox (eq 1b). Such formation and dispersion cycles of the chiral π-dimer complex in response to ET reduction and oxidation are highly reversible and it can be repeated many times as shown in Figure 2.

Formation of $(Q^{\bullet-})_2-(Sc^{3+}(R)\text{-pybox})_2$ was examined by ^{1}H NMR (see Supporting Information S5).[19] The ^{1}H COSY NMR spectrum of the 1:1:1 mixture of a deaerated CD_3CN solution of Me_2Fc, Q, and Sc^{3+}(*R*)-pybox is shown in Figure 3a.[22,23] Deuterium substitution of Q by Q-d_4 results in disappearance of two doublet peaks: ^{1}H NMR (CD_3CN) δ 4.94 (d, $J = 8.4$ Hz) and δ 4.09 (d, $J = 8.4$ Hz) as shown in Figure 3b. This indicates that those are individual protons in $(Q^{\bullet-})_2$ of $(Q^{\bullet-})_2-(Sc^{3+}(R)\text{-pybox})_2$.

The optimized structure of $(Q^{\bullet-})_2-(Sc^{3+}(R)\text{-pybox})_2$ is calculated by using density functional theory (DFT) at the B3LYP/6-31G* basis [Figure 3d (top view) and 3e (front view)]. There are different sets of protons termed H_A and H_B in $(Q^{\bullet-})_2$, where H_B is shielded as compared with H_A by phenyl rings of (*R*)-pybox. This is consistent with two doublet peaks in the ^{1}H NMR spectrum (Figure 3a). NOE are detected between H_B (or H_A) protons and phenyl protons of Sc^{3+}(*R*)-pybox (termed *a*) when irradiated at H_B as shown in Figure 3c.[24] This indicates that Sc^{3+}(*R*)-pybox is located near $(Q^{\bullet-})_2$, supporting the suggested structure of $(Q^{\bullet-})_2-(Sc^{3+}(R)\text{-pybox})_2$.

The enantiomer pairs of $(Q^{\bullet-})_2$ in $(Q^{\bullet-})_2-(Sc^{3+}\text{-pybox})_2$ without Sc^{3+}-pybox are shown in Figure 3f, in which individual protons are distinguished by blue and green. Those enantiomer pairs are non-superimposable mirror images of each other. Such mirror symmetry breaking in the $(Q^{\bullet-})_2$ unit through the chiral π-dimer complex formation should cause the induced circular dichroism (ICD) in the long wavelength region (Figure 1b,c). In the case of monomer radical anion $Q^{\bullet-}$, however, the enantiomer pairs are superimposable mirror images. Thus, dimer formation of $Q^{\bullet-}$ plays a crucial role in supramolecular chirogenesis.

In conclusion, we have developed chiral assemblies responding to ET. New frontiers of chiral assemblies will be exploited in such ET controlled chiral assembly systems.

Acknowledgment. This work was partially supported by Grants-in-Aid (Nos. 19205019) from the Ministry of Education, Culture, Sports, Science and Technology, Japan.

Supporting Information Available: Schematic molecular orbital diagrams for π-dimers (S1), UV−vis and ^{1}H NMR titration (S2), the oxidation of $(NQ^{\bullet-})_2-(Sc^{3+}(R)\text{-pybox})_2$ by DDQ (S3), estimation of the association constants for the chiral π-dimer complexes (S4), ^{1}H NMR spectra of $(Q^{\bullet-})_2-(Sc^{3+}(R)\text{-pybox})_2$ (S5), NOESY NMR spectrum of $(NQ^{\bullet-})_2-(Sc^{3+}(R)\text{-pybox})_2$ (S6), and ESR spectra of the paramagnetic monomer complexes (S7).

References

(1) Scarso, A.; Rebek, J., Jr. In *Topics in Current Chemistry*: *Supramolecular Chirality*; Crego-Calama, M., Reinhoudt, D. N., Eds.; Springer-Verlag: Berlin, 2006; Vol. 265, pp 1−46.
(2) Brandt, U. *Annu. Rev. Biochem.* **2006**, *75*, 69.
(3) Stowell, M. H. B.; McPhillips, T. M.; Rees, D. C.; Soltis, S. M.; Abresch, E.; Feher, G. *Science* **1997**, *276*, 812.
(4) Conn, M. M.; Rebek, J., Jr. *Chem. Rev.* **1997**, *97*, 1647.
(5) Casnati, A.; Sansone, F.; Ungaro, R. *Acc. Chem. Res.* **2003**, *36*, 246.
(6) Prins, L. J.; De Jong, F.; Timmerman, P.; Reinhoudt, D. N. *Nature* **2000**, *408*, 181.
(7) Yashima, E.; Maeda, K.; Okamoto, Y. *Nature* **1999**, *399*, 449.
(8) Swiegers, G. F.; Malefetse, T. J. *Chem. Rev.* **2000**, *100*, 3483.
(9) Leininger, S.; Olenyuk, B.; Stang, P. J. *Chem. Rev.* **2000**, *100*, 853.
(10) Caulder, D. L.; Raymond, K. N. *Acc. Chem. Res.* **1999**, *32*, 975.
(11) Piguet, C.; Bernardinelli, G.; Hopfgartner, G. *Chem. Rev.* **1997**, *97*, 2005.
(12) For redox control of 1:1 host−guest interactions and molecular motions in supramolecular systems see: (a) Kaifer, A. E. *Acc. Chem. Res.* **1999**, *32*, 62. (b) Collin, J.-P.; Dietrich-Buchecker, C.; Gaviña, P.; Jimenez-Molero, M. C.; Sauvage, J.-P. *Acc. Chem. Res.* **2001**, *34*, 477. (c) Bissell, R. A.; Cordova, E.; Kaifer, A. E.; Stoddart, J. F. *Nature* **1994**, *369*, 133.
(13) *Functions of Quinones in Energy Conserving Systems*; Trumpower, B. I., Ed.; Academic Press: New York, 1986.
(14) [Sc-pybox](OTf)$_3$ has been extensively utilized in enantioselective rare-earth catalyzed quinone Diels-Alder reactions see: Evans, D. A.; Wu, J. *J. Am. Chem. Soc.* **2003**, *125*, 10162.
(15) For highly self-organized ET in the Sc^{3+}-promoted ET reduction of Q due to the formation of π-dimer radical anion complexes of Q bridged by two and three Sc^{3+} $[Q^{\bullet-}-(Sc^{3+})_n-Q, n = 2, 3]$ see: Yuasa, J.; Suenobu, T.; Fukuzumi, S. *J. Am. Chem. Soc.* **2003**, *125*, 12090.
(16) For the complex between organic radical anions and transition metals see: Ernst, S.; Hänel, P.; Jordanov, J.; Kaim, W.; Kasack, V.; Roth, E. *J. Am. Chem. Soc.* **1989**, *111*, 1733.
(17) (a) Feringa, B. L.; van Delden, R. A.; Koumura, N.; Geertsema, E. M. *Chem. Rev.* **2000**, *100*, 1789. (b) Borovkov, V. V.; Hembury, G. A.; Inoue, Y. *Acc. Chem. Res.* **2004**, *37*, 449.
(18) The absorption band due to the semiquinone radical anion dimers without Sc^{3+} are known to appear in the long wavelength region as compared with the absorption band due to the monomer radical anions see: Lü, J.-M.; Rosokha, S. V.; Kochi, J. K. *J. Am. Chem. Soc.* **2003**, *125*, 12161.
(19) Absorption band in the long wavelength region and the diamagnetic character of $(Q^{\bullet-})_2-(Sc^{3+}(R)\text{-pybox})_2$ [or $(NQ^{\bullet-})_2-(Sc^{3+}(R)\text{-pybox})_2$] may result from formation of a π-bonding orbital between two $Q^{\bullet-}$ (or $NQ^{\bullet-}$) molecules (see schematic molecular orbital diagrams for the chiral π-dimer complexes in Supporting Information S1).
(20) ET from Me_2Fc to Q and NQ becomes possible by the presence of Sc^{3+}-pybox. This indicates the large association constants of the chiral π-dimer complexes (see Supporting Information S4).
(21) Fukuzumi, S. *Org. Biomol. Chem.* **2003**, *1*, 609.
(22) For ^{1}H NMR spectrum of $(NQ^{\bullet-})_2-(Sc^{3+}(R)\text{-pybox})_2$ (see Supporting Information S6).
(23) The diamagnetic chiral π-dimer complexes, $(Q^{\bullet-})_2-(Sc^{3+}(R)\text{-pybox})_2$ and $(NQ^{\bullet-})_2-(Sc^{3+}(R)\text{-pybox})_2$ are also in equilibrium with the paramagnetic monomer complexes, $Q^{\bullet-}-Sc^{3+}(R)$-pybox and $NQ^{\bullet-}-Sc^{3+}(R)$-pybox, respectively (see Supporting Information S7). However, the concentrations of these complexes are extremely small (<0.07%) as compared with those of the diamagnetic chiral π-dimer complexes.
(24) The $(Q^{\bullet-})_2$ moiety in the complex is exchanged with Q and QH_2 in the NOE time scale. This leads to exchange between H_A and H_B.

JA075149Q